Electronic Supplementary Material (ESI) for ChemComm.
This journal is © The Royal Society of Chemistry 2018

Electronic Supplementary Information

P-doped carbons derived from cellulose as a highly efficient metal-free catalyst for aerobic oxidation of benzyl alcohol in water under air atmosphere

Zhouyang Long, [†a] Liming Sun, [†a] Weijie Zhu,[a] Guojian Chen,[*a] Xiaochen Wang[b] and Wen Sun[c]

[a] School of Chemistry and Materials Science, Jiangsu Key Laboratory of Green Synthetic Chemistry for Functional Materials, Jiangsu Normal University, Xuzhou 221116, China

[b] Department of Chemistry and Materials Engineering, Hefei University, Hefei 230022, Anhui, China

[c] State Key Laboratory of Fine Chemicals, Dalian University of Technology, Dalian 116024, China

† These authors contributed equally to this work

** Corresponding author, E-mail: gjchen@jsnu.edu.cn*

Experimental

Material and methods

All solvents and reagents were purchased from commercial source and used without further purification. XRD patterns were collected on the Bruker D8 Advance powder diffractometer using Ni-filtered Cu Ka radiation source at 40 kV and 20 mA, from 5 to 90° with a scan rate of 0.2° s^{-1}. Raman spectrum was collected on a Raman spectrometer (Jobin Yvon Labram HR800) with 532-nm laser. Field emission scanning electron microscope (FESEM; Hitachi SU8010, accelerated voltage: 15 kV) was used to study the morphology of the catalysts and the element distribution. The Brunauer-Emmett-Teller (BET) surface area and pore structure of the samples were obtained by nitrogen adsorption-desorption isotherm measurements (Quantachrome autosorb iQ2). Fourier transform infrared (FT-IR) spectra were recorded on a Bruker Vertex 80V instrument (KBr disks) in the 4000-500cm^{-1} region. Contact angles were measured with a contact angle meter (DropMeter A-100P) at 25 °C. The contact angles were measured according to the powder compressing method.[S1] The catalyst was compressed at 20 tons pressure during 1 min and the contact angles were determined by depositing 5 μL liquid onto the compressed pellet. The surface states were analyzed by X-ray photoelectron spectroscopy (XPS, AXIS-NOVA, Kratos Inc.) using an X-ray source of mono-chromatic Al Ka (1486.6 eV) 150 W.

Preparation of catalysts

The P-doped carbon catalysts were prepared by carbonizing the H_3PO_4-activated microcrystalline cellulose via a similar method in the reported works.[17,19] Firstly, 4.0 g microcrystalline cellulose was dispersed in 15 mL water, then pre-weighed phosphoric acid (H_3PO_4, 85 wt%) was added. The weight ratio of microcrystalline cellulose to H_3PO_4 (85 wt%) was X:1 (M= 32, 16, 8, 4). The resulting mixtures were stirred at room temperature for 24 h, and then dried at 80 ^{o}C in a drying oven. Secondly, the obtained solids were transferred into a quartz boat and calcined in a pipe furnace under N_2 atmosphere at a rate of 10 ^{o}C/min to reach the temperature of T ^{o}C (T=700, 800 or 900) and kept at T ^{o}C for 2 h. The samples were cooled to room temperature naturally, washed with water for three times and dried at 100 ^{o}C. The obtained catalysts were labelled as MCel-PC-X(T), which denotes the microcrystalline cellulose derived P-doped carbon prepared with the mass ratio of microcrystalline cellulose to H_3PO_4 (85%) being X:1.

Pure carbon catalyst MCel-C was prepared from microcrystalline cellulose without adding H_3PO_4 (85 wt%).

Catalytic reaction process

The catalytic performances of the prepared catalysts were tested for liquid phase aerobic oxidation of alcohols. The reaction runs were conducted in a 100 mL thick-walled glass pressure bottle (Fig. S1A), which was loaded with 1 mmol BA, 0.1 g catalyst, and 1 mL water (solvent) and closed. The self-contained static air in the bottle was used as the oxidant. The bottles were placed in a parallel reactor (Fig. S1B) and the reactions went at the specified temperature with 350 rpm stirrer speed for a specified time. After the reaction, the solid catalyst was isolated by centrifugation and the liquid mixture was analysed by a gas chromatograph. The recycled catalyst was washed with ethanol for three times and acetone for three times before being dried in a vacuum oven at 80 ^{o}C. The recovered catalyst was used for the next run without adding any fresh catalyst.

Theoretical calculations

Periodic density functional theory (DFT) computations were performed by using a plane-wave method implemented in the Cambridge Sequential Total Energy Package (CASTEP) code.[S2] The exchange-correlation potential was described by generalized gradient approximation with the Perdew-Burke-Ernzerhof (GGA-PBE) scheme.[S3] Interaction between the valence electrons and the ion core was substituted by an ultrasoft pseudopotential.[S4] A 300eV cutoff for the plane-wave basis set was adopted in all computations. The self-consistent convergence accuracy was set at 2×10^{-5} eV/atom, the convergence criterion for the force between atoms was 0.05eV/Å, and the maximum displacement was 0.002Å.

The binding energies between three P species and BA were obtained according to the following equation:

$$E_b = E_{com} - E_P - E_{BA}$$

where E_{com}, E_P and E_{BA} represent the total energies of the relaxed P species/BA composite, pure P species and BA, respectively.

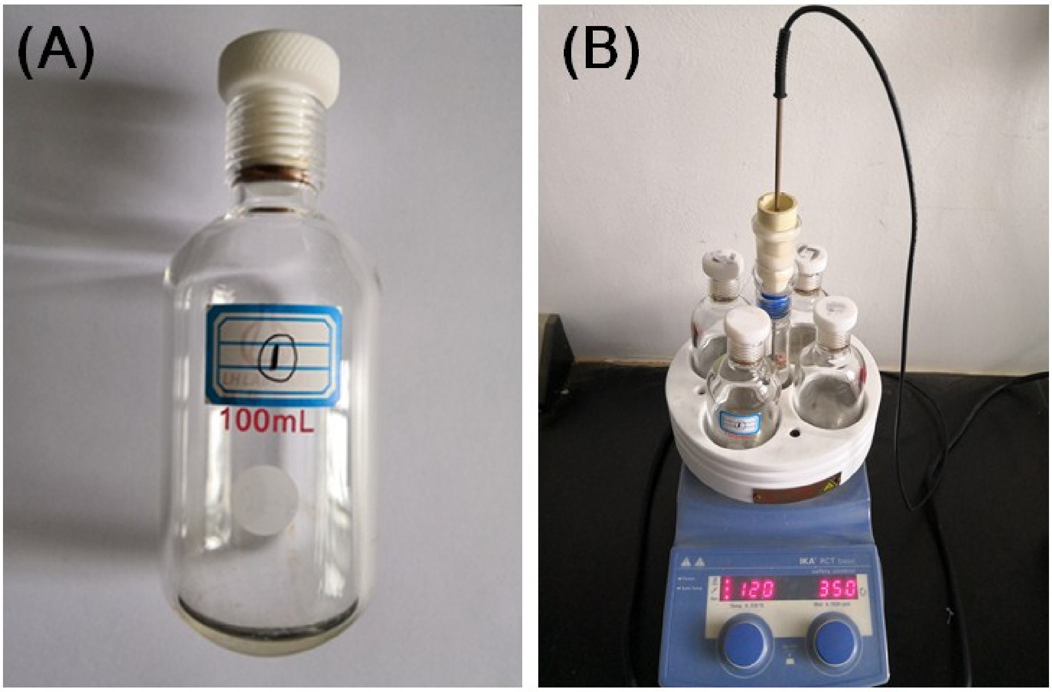

Fig. S1. The glass pressure bottle and parallel reactor used in the present work.

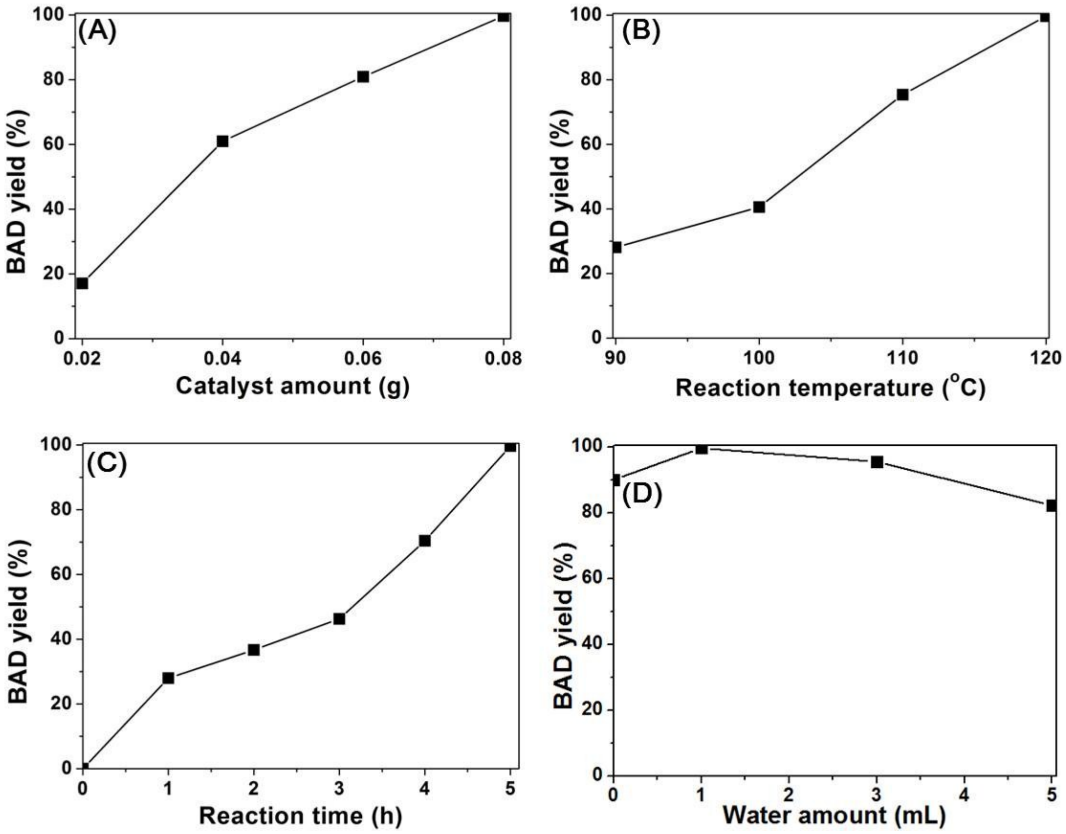

Fig. S2. Effects of reaction parameters on the yield of BAD. (A) amount of catalyst (B) reaction temperature, (C) reaction time and (D) amount of water.

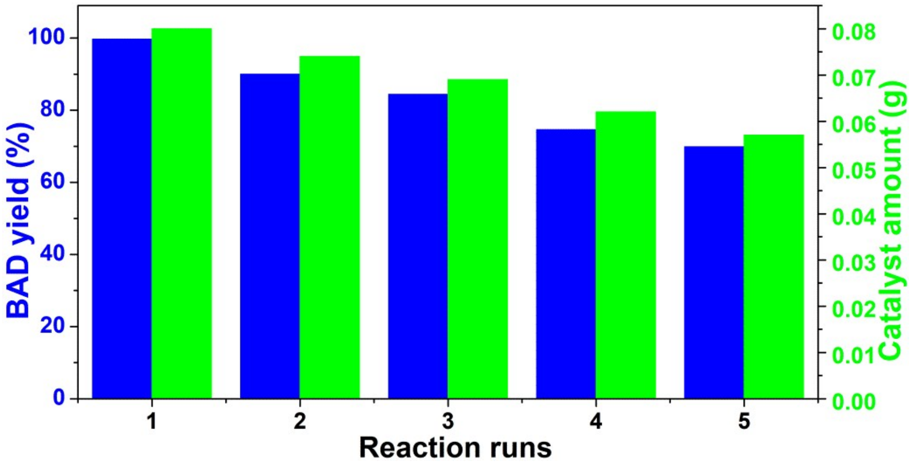

Fig. S3. Recycling the MCel-PC-4(800) for the selective aerobic oxidation of BA to BAD. Reaction conditions: 1 mmol BA, 1 mL water, T=120 °C, t=5 h. Blue bar: the BAD yield; Green bar: the catalyst amount.

Fig. S3 displays the result of a five-run test for the catalytic reusability of the MCel-PC-4(800). The recovered catalyst is weighed to be 0.074 g for the 2nd, 0.069 g for the 3rd, 0.062 g for the 4th and 0.057 g for the 5th run, with the recovery ratios being 92.5, 86.3, 77.5 and 71.3 wt% based on 0.08 g, respectively. The catalyst loss is inevitable during the recovery operation procedure although carefulness is paid. Without additional fresh catalyst, the BAD yield is 90.0% for the second run, 84.4%, 74.6% and 69.9% for the following runs. It is obvious that the decline degree of the BAD yield is very close to the loss degree of the catalyst in each run. The TOF value for the five runs are 24.9×10^{-4}, 24.3×10^{-4}, 24.5×10^{-4}, 24.1×10^{-4} and 24.5×10^{-4} mol benzaldehyde / (g catalyst × h reaction time), respectively, implying that the activity of the recovered catalysts for converting BA to BAD is stable in the recycling test. Therefore, the decline of catalyst amount due to recovery operation may be responsible for the decrease of the BAD yield shown in Fig. S3.

The hot filtration test is conducted by a similar method in a recently reported work.[S5] The mixture of the solid catalyst and the solvent water is heated at 120 °C for 2 h, and then the mixture is filtrated when it is hot. A little water is added into the filtrate to make its volume as 1 mL. Then the filtrate is put back into the reactor and 1 mmol benzyl alcohol is added. After 5 h at 120 °C, the reaction mixture is analyzed by GC and trace amount of benzaldehyde (< 0.1% yield) is observed, which is similar with the reaction result from the blank test in the absence of the catalyst. Therefore, the leaching of the doped-P species, if any, is negligible.

Table S1. Comparison of this work with previous similar reports for selective aerobic oxidation of BA to BAD.

Cat.	**BA used (mmol)**	**Loading[a] (wt%)**	**Oxidant**	**T (^oC)**	**t (h)**	**Solvent (V mL)**	**Y (%)**	**S (%)**	**TOF ($\times10^{-4}$)**	**Ref.**
MCel-PC-4(800)	1.0	74	air	120	5	Water (1)	99.7	99.9	24.9	This work
MCel-PC-4(800)	1.0	74	air	120	5	--	90.1	99.9	22.5	This work
GO	1.9	50	air	150	24	--	84.2	86.9	6.7	[10]
NG	0.1	278	O_2	70	10	Water (80)	12.8	100	0.4	[11]
N-AC	1.1	84	air	120	5	Ethanol (5)	23	100	5.1	[12]
PGc	1.0	50	O_2	100	24	--	53.7	95.7	4.8	[13]
PS-Gc	1.0	50	O_2	100	24	--	53.6	91.0	5.8	[14]
PS-Gc	0.5	50	air	100	24	--	30.6	97.4	2.6	[14]

[a] The value of $m_{BA}/m_{catalyst}$

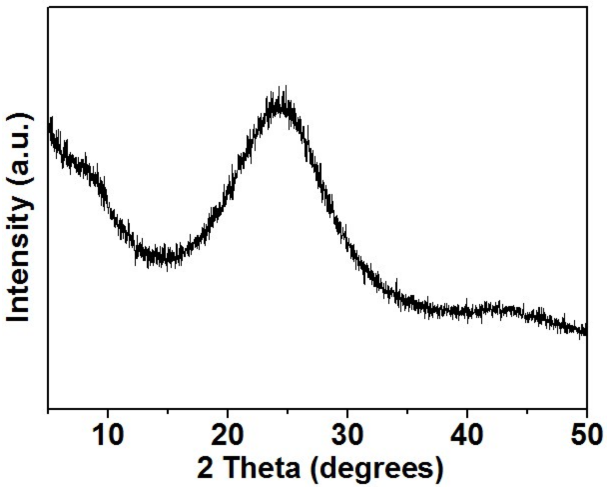

Fig. S4. XRD pattern of MCel-PC-4(800).

Fig. S4 shows the wide-angle XRD pattern of the MCel-PC-4(800). It can be seen that the MCel-PC-4(800) only exhibits a broad peak centred at about 24^{o}, indicating that the MCel-PC-4(800) is amorphous.[10-14]

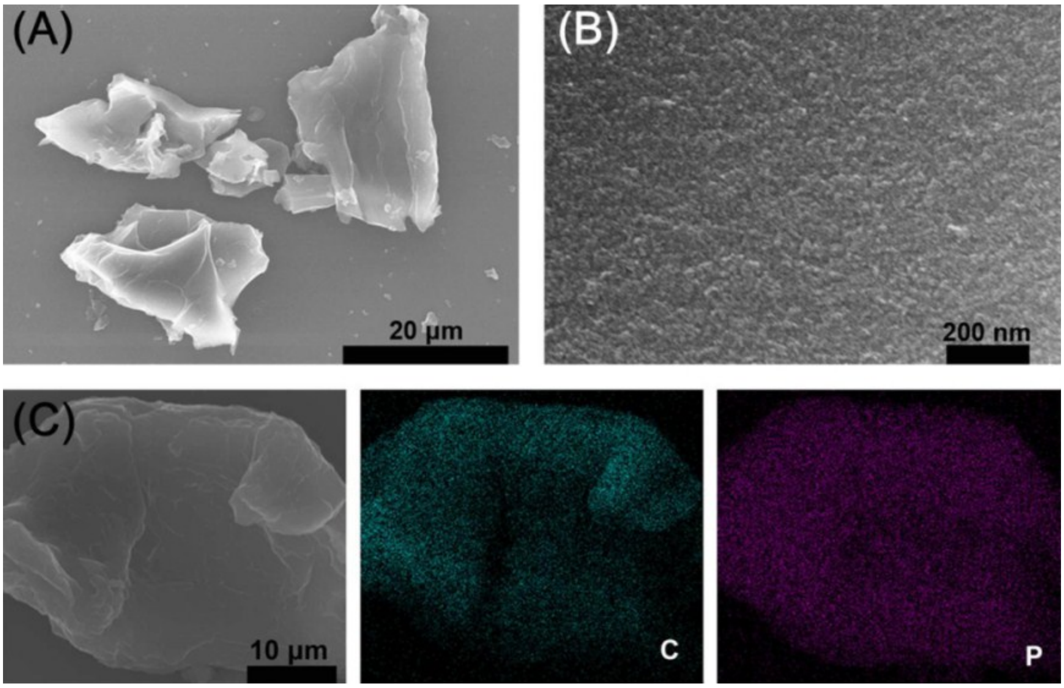

Fig. S5. (A) and (B) SEM images of MCel-PC-4(700); (C) EDS elemental (C and P) mapping images of MCel-PC-4(700).

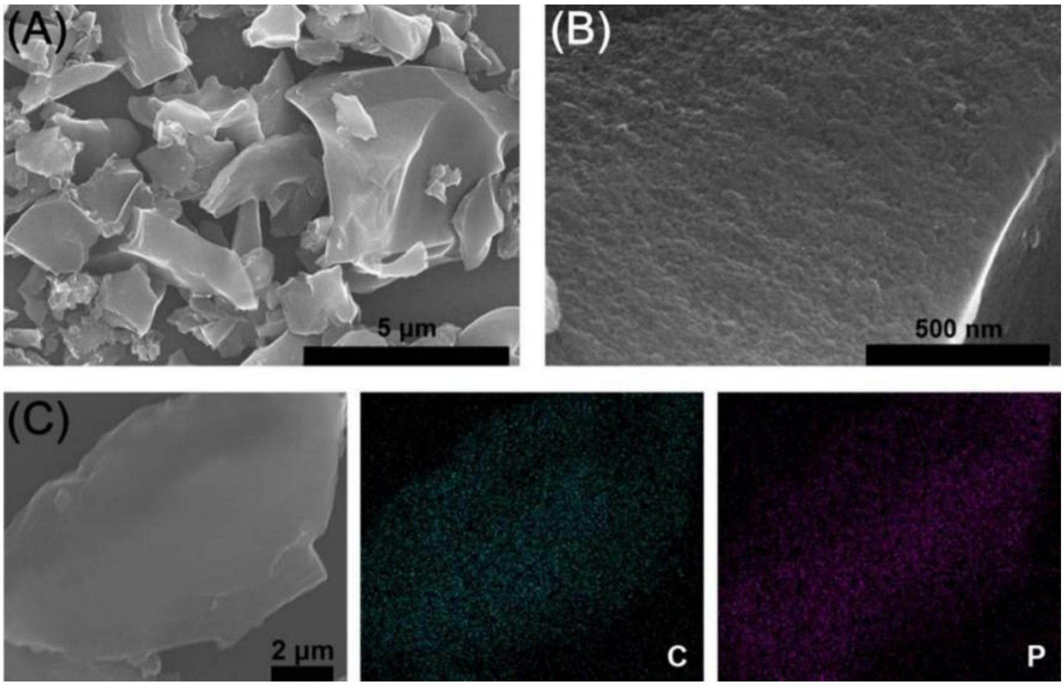

Fig. S6. (A) and (B) SEM images of MCel-PC-4(800); (C) EDS elemental (C and P) mapping images of MCel-PC-4(800).

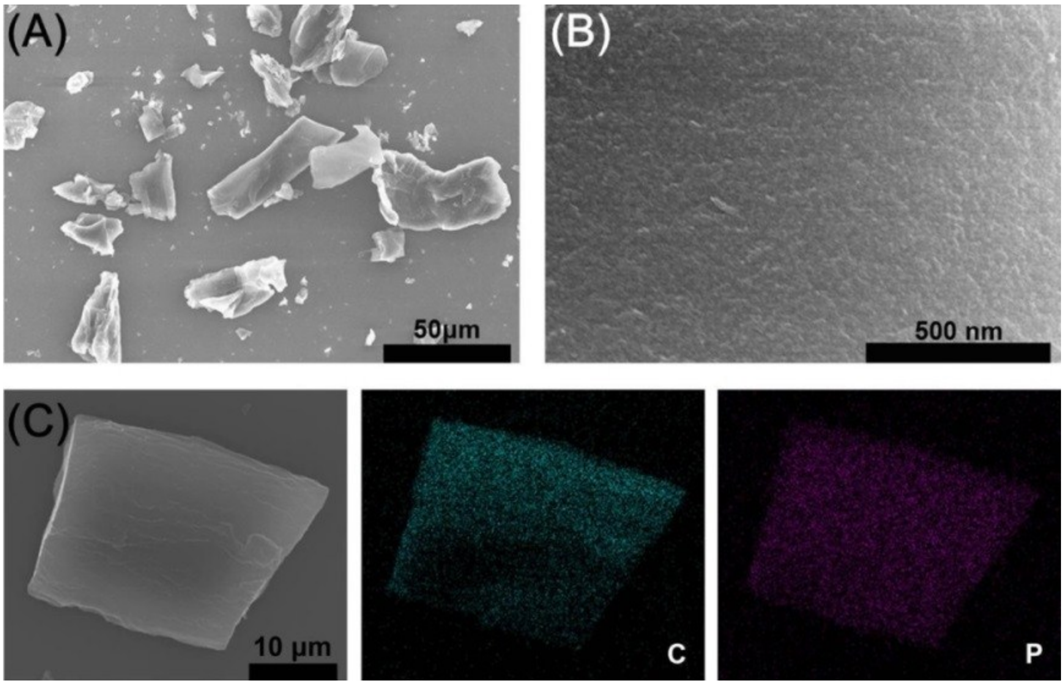

Fig. S7. (A) and (B) SEM images of MCel-PC-4(900); (C) EDS elemental (C and P) mapping images of MCel-PC-4(900).

Fig. S5-S7 display the scanning electron microscopy (SEM) images and elemental mappings of the three MCel-PC4 catalysts. Fig. S5A, S6A and S7A exhibit general morphologies of the samples, showing irregular bulk shapes with the size of several micrometers. As can be seen in the magnified image in Fig. S5B, S6B and S7B, the surfaces of the three MCel-PC4 catalysts are rather rough, with small pits and holes existing. Furthermore, elemental mappings (S5C, S6C and S7C) are performed to obtain more composition information. The mapping images indicate that the phosphorus are homogeneously distributed in the three MCel-PC4 catalysts.

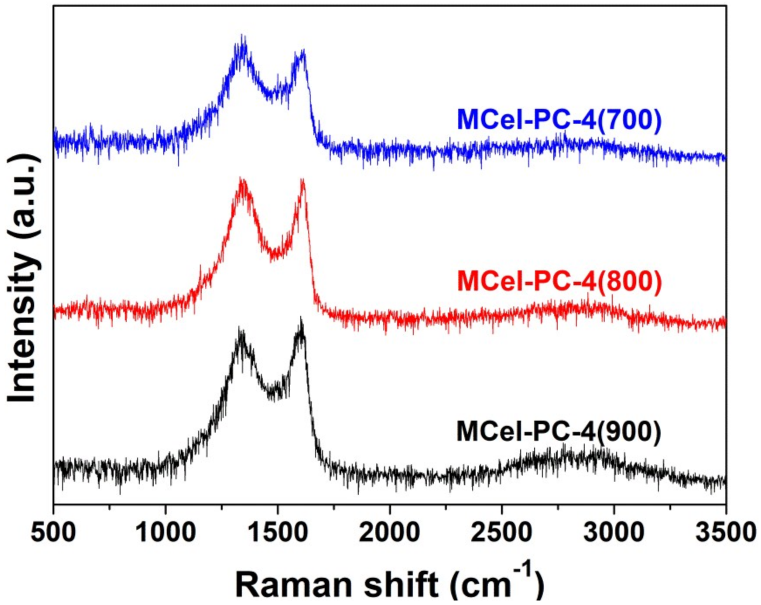

Fig. S8. Raman spectra of the MCel-PC-4(700), MCel-PC-4(800) and MCel-PC-4(900) catalysts.

Raman spectra of the three MCel-PC-4(T)s samples are depicted in Fig. S8 where two prominent peaks centered around 1339 and 1605 cm^{-1} are observed, representing the characteristic D and G bands of carbon materials, respectively.[S6-S9] The D band indicates the presence of disordered graphite structure, while the G band is indicative of the crystalline graphitic carbon in the MCel-PC-4(T)s.[S6-S9] Besides, the intensity ratio of the D and G bands (I_D/I_G) of MCel-PC-4(T)s is estimated to be 2.17, 1.85 and 1.70 for MCel-PC-4(700), MCel-PC-4(800) and MCel-PC-4(900), respectively, which becomes smaller along with the increase of temperature. This suggests that increasing the carbonization temperature lead to the improved graphitization and less disordered carbon atoms.[17,S6,S8]

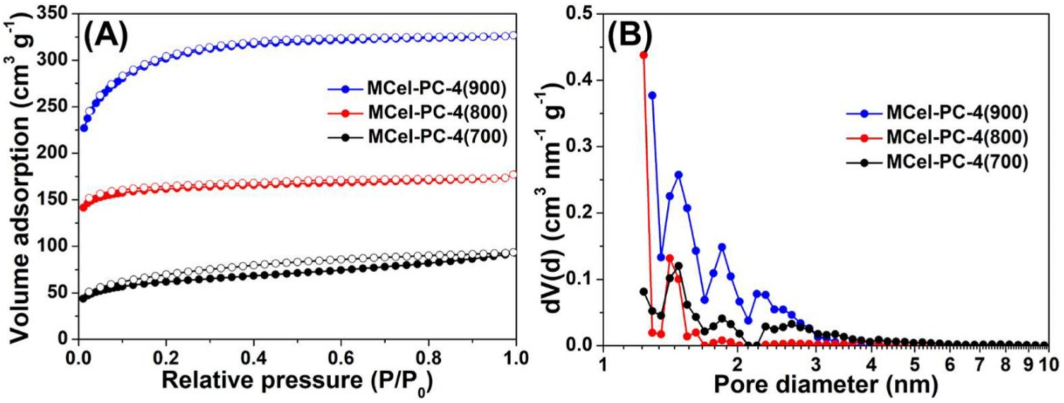

Fig. S9. (A) N_2 adsorption-desorption isotherms and (B) NLDFT pore size distributions of the MCel-PC-4(700), MCel-PC-4(800) and MCel-PC-4(900).

As can be seen in Fig. S9(A), the N_2 adsorption isotherms of the three MCel-PC-4s are type I, according to the classification of the IUPAC,[S10] indicating the microporous character of MCel-PC-4s. The pore size distributions curve in Fig. S9(B) give their most probable pore sizes centered from 1.23 nm to 1.85 nm calculated by using a slit/cylindrical NLDFT model. Furthermore, it can be seen in Table S2 that the BET surface areas for the three MCel-PC-4s are 231 m^2 g^{-1} for MCel-PC-4(700), 641 m^2 g^{-1} for MCel-PC-4(800) and 1131 m^2 g^{-1} for MCel-PC-4(900). It is likely that a higher carbonization temperature leads to a larger BET surface area. Generally, large BET surface area facilitates the mass transfer process in the heterogeneous catalysis. However, MCel-PC-4(900) which has the largest BET surface area exhibits the lowest catalytic activity. Hence, it is reasonable to propose that the BET surface area is not the dominant factor to determine the activity of the present catalyst.

Table S2. Textural properties and P contents of the MCel-PC-4(700), MCel-PC-4(800) and MCel-PC-4(900).

Entry	Sample	P content (at%)[a]	S_{BET} (m^2 g^{-1})[b]	V_{total} (cm^3 g^{-1})[c]	D_p (nm)[d]
1	MCel-PC-4(700)	3.31	231	0.14	1.23, 1.48
2	MCel-PC-4(800)	2.84	641	0.27	1.23, 1.41
3	MCel-PC-4(900)	1.88	1131	0.51	1.29, 1.47, 1.85

[a] The tested P atomic concentrations of X-ray photoelectron spectroscopy data (XPS). [b] BET surface area calculated over the range P/P_0=0.05~0.20. [c] Total pore volume calculated at P/P_0=0.99. [d] The peak pore diameter calculated by the NLDFT theory.

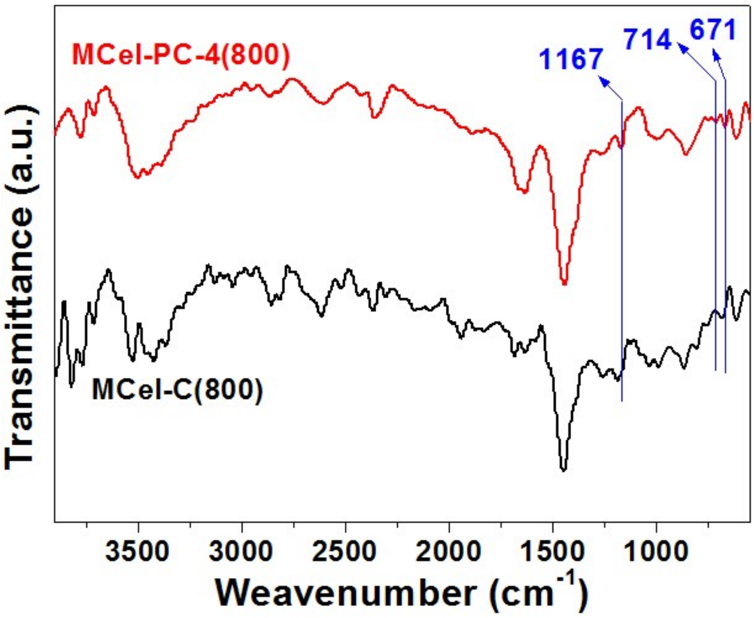

Fig. S10. FT-IR spectra of MCel-PC-4(800) and MCel-C(800).

The FT-IR spectra of MCel-PC-4(800) and MCel-C(800) are shown in Fig. S10. Compared with the P-free MCel-C(800), there are three more vibrations at 671, 714 and 1172 cm^{-1} for the P-doped MCel-PC-4(800). The former two at 671 and 714 cm^{-1} are attributed to the P-C stretching and the last one at 1172 cm^{-1} is attributed to the P=O stretching in the MCel-PC-4(800).[13]

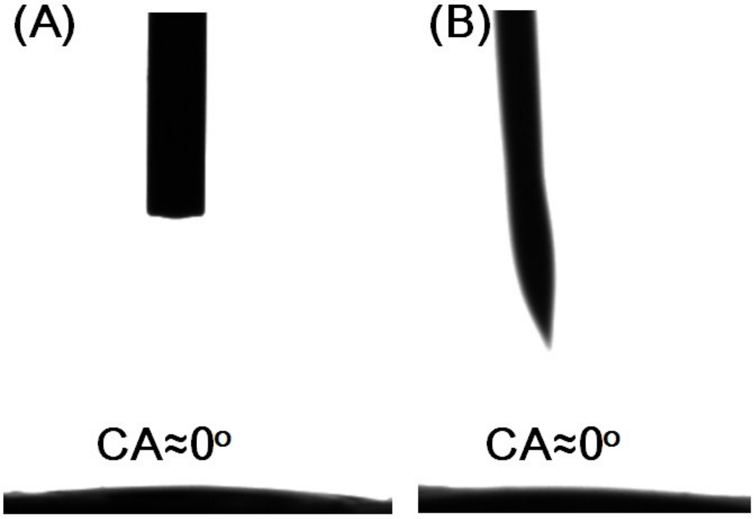

Fig. S11. Contact angles of (A) water droplet and (B) benzyl alcohol droplet on the surface of MCel-PC-4(800).

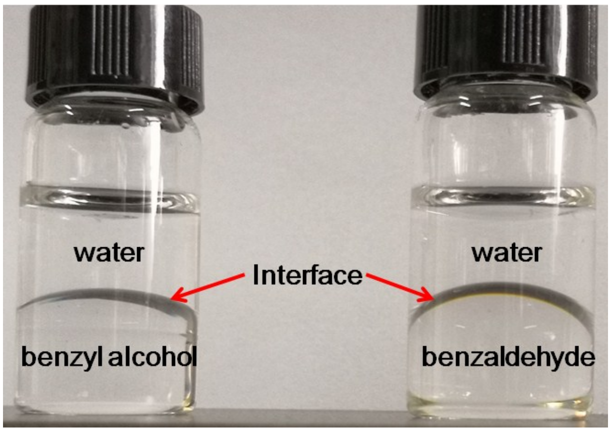

Fig. S12. The mixture of benzyl alcohol/water (left) and the mixture of benzaldehyde/water (right).

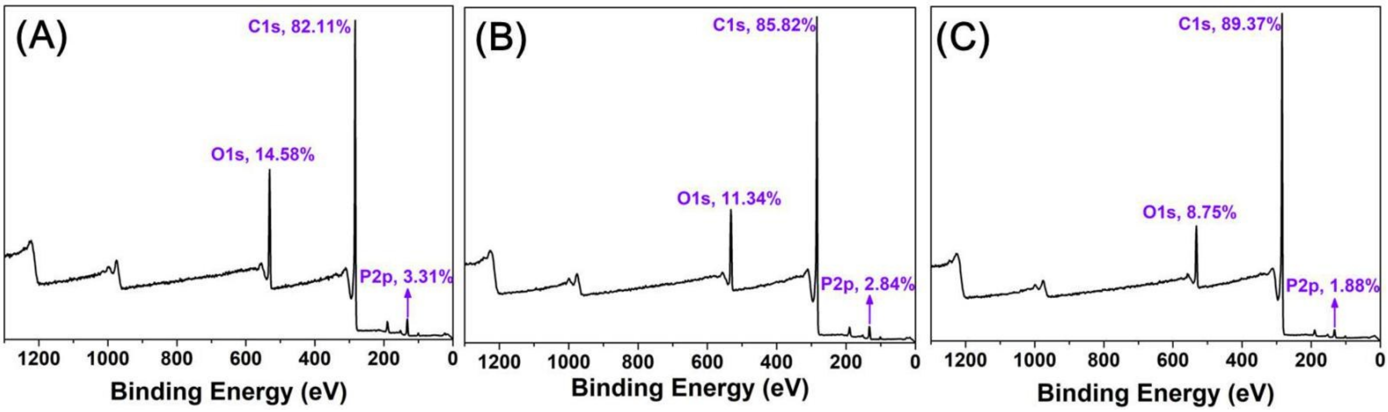

Fig. S13. XPS survey spectra of the (A) MCel-PC-4(700), (B) MCel-PC-4(800) and (C) MCel-PC-4(900) catalysts.

The XPS survey spectra of the three MCel-PC-4 samples (Fig. S13) show strong carbon C1 s peaks at about 283.6 eV as well as signals for oxygen O1 s at 531.5 eV and phosphorus P 2p at around 133.0 eV. It can be seen that with the carbonization temperature increases from 700 ^{o}C to 800 ^{o}C and 900 ^{o}C, the C content of the three MCel-PC-4 catalysts increase from 82.11% to 85.82% and 89.37%, while the O and P contents decrease from 14.58% to 11.34% and 8.75%, 3.31% to 2.84% and 1.88% , respectively.

Table S3. The doped-P species of the MCel-PC-4(T), where T=700, 800, and 900 (the carbonization temperature, ^{o}C).

Entry	Catalyst	The total P content (at %)[a]	The P species categories and corresponding contents relative amount / absolute content		
			$C\text{-}O\text{-}PO_3$ (134.2±0.2 eV)	$C\text{-}PO_3$ (133.4±0.2 eV)	C_3PO (132.5±0.1 eV)
1	MCel-PC-4 (700)	3.31	43.3% / 1.433%	37.5% / 1.241%	19.2% / 0.636%
2	MCel-PC-4 (800)	2.84	36.4% / 1.034%	36.6% / 1.039%	27.0% / 0.767%
3	MCel-PC-4 (900)	1.88	36.0% / 0.677%	34.0% / 0.639%	30.0% / 0.564%

[a] X-ray photoelectron spectroscopy data (XPS).

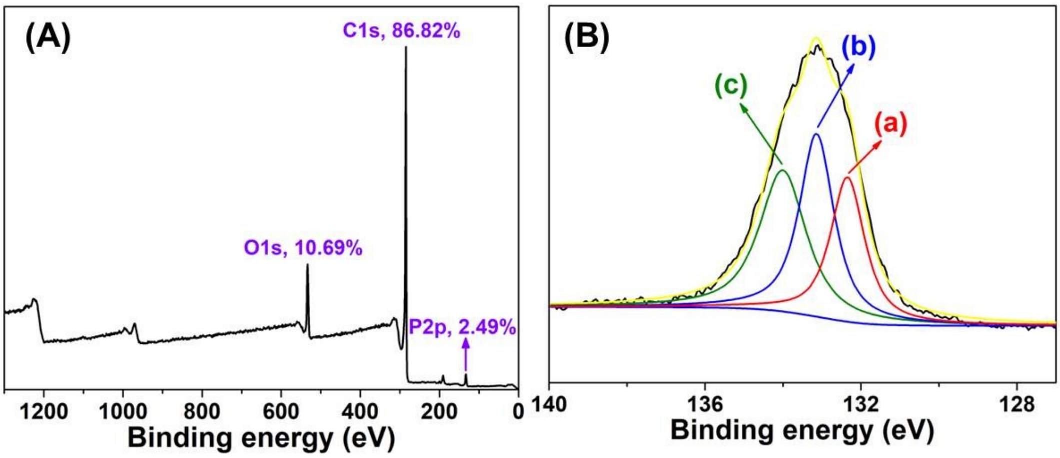

Fig. S14. (A) XPS survey spectrum of the recovered MCel-PC-4(800) catalyst. (B) P 2p spectrum for the recovered MCel-PC-4(800) catalyst, (a) C_3PO, (b) C-PO_3 and (c) C-O-PO_3.

It can be seen that the total P contents in the recovered catalyst is 2.49%, lower than the one of 2.84% for the fresh catalyst, indicating a slight loss of the doped-P species. The slight loss of the doped-P species may be an additional cause for the decline of the BAD yield in the reusability test.

Table S4. The doped-P species of the recovered MCel-PC-4(800).

Catalyst	The total P content (at %)[a]	The P species categories and corresponding contents relative amount / absolute content		
		C-O-PO_3 (134.0 eV)	C-PO_3 (133.1 eV)	C_3PO (132.3 eV)
Recovered MCel-PC-4 (800)	2.49	36.8% / 0.916%	35.6% / 0.886%	27.6% / 0.687%

[a] X-ray photoelectron spectroscopy data (XPS).

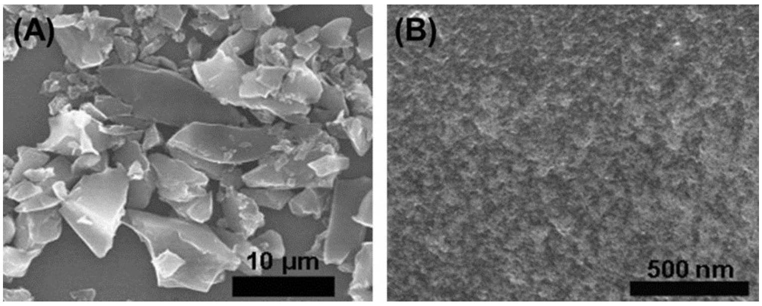

Fig. S15. SEM images of the recovered MCel-PC-4(800).

It can be seen that the morphology of the recovered catalyst is similar with the fresh one.

Table S5. The bond length of P=O bonds and the Mulliken Charge Population on P, O atoms and P=O bonds for C_3PO, $C\text{-}PO_3$, and $C\text{-}O\text{-}PO_3$ species.

	charge population			length (Å)
	P	O	P=O bond	P=O bond
C_3PO	1.68	-0.92	0.82	1.469
$C\text{-}PO_3$	2.25	-1.01	0.88	1.457
$C\text{-}O\text{-}PO_3$	2.45	-1.03	0.90	1.450

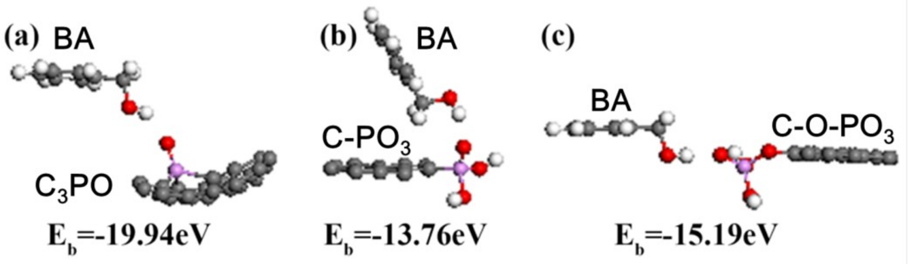

Fig. S16. Models for simulating the adhesion between three P species and BA after geometry optimization: (a) C_3PO/BA; (b) $C\text{-}PO_3$/BA; and (c) $C\text{-}O\text{-}PO_3$/BA.

References

[S1] M. Lazghab, K. Saleh, I. Pezron, P. Guigon and L. Komunjer, *Powder Technol.*, 2005, **157**, 79-91.

[S2] S.J. Clark, M.D. Segall, C.J. Pickard, P.J. Hasnip, M.J. Probert, K. Refson and M.C. Payne, *Z. Kristallogr.*, 2005, **220**, 567.

[S3] J.P. Perdew, K. Burke and M. Ernzerhof, *Phys. Rev. Lett.*, 1996, **77**, 3865.

[S4] A.M. Rappe, K.M. Rabe, E. Kaxiras and J.D. Joannopoulos, *Phys. Rev. B*, 1990, **41**, 1227.

[S5] M. Gholinejad, F. Zareh and C. Nájera, *Appl. Organomet. Chem.* 2018, **32**, e3984

[S6] C. L. Chen, J. Zhang, B. S. Zhang, C. L. Yu, F. Peng and D. S. Su, *Chem. Commun.*, 2013, **49**, 8151.

[S7] F. P. Pan, Z. Y. Cao, Q. P. Zhao, H. Y. Liang, J. Y. Zhang, *J. Power Sources*, 2014, **272**, 8.

[S8] X. Lin, Z. Z. Nie, L. Y. Zhang, S. C. Mei, Y. Chen, B. S. Zhang, R. L. Zhu and Z. G. Liu, *Green Chem.*, 2017,**19**, 2164.

[S9] Y. H. Cao, H. Yu, J. Tan, F. Peng, H. J. Wang, J. Li, W. X. Zheng and N.-B. Wong, *Carbon*, 2013, **57**, 433.

[S10] K.S.W. Sing, D.H. Everett, R.A.W. Haul, L. Moscou, R.A. Pierotti, J. Rouquerol and T. Siemieniewska, *Pure Appl. Chem.*, 1985, **57**, 603.